Formation and evolution of bubbly screens in confined oscillating bubbly liquids

Sergey Shklyaev

Department of Theoretical Physics, Perm State University, Bukirev 15, Perm 614990, Russia
and Department of Physics and Astronomy, University of Potsdam, Karl-Liebknecht-Straße 24/25, D-14476 Potsdam-Golm, Germany

Arthur V. Straube*

Department of Physics, Humboldt University of Berlin, Newtonstr. 15, D-12489 Berlin, Germany
and Department of Physics and Astronomy, University of Potsdam, Karl-Liebknecht-Straße 24/25, D-14476 Potsdam-Golm, Germany

We consider the dynamics of dilute monodisperse bubbly liquid confined by two plane solid walls and subject to small-amplitude high-frequency oscillations normal to the walls. The initial state corresponds to the uniform distribution of bubbles and motionless liquid. The period of external driving is assumed much smaller than typical relaxation times for a single bubble but larger than the period of volume eigenoscillations. The time-averaged description accounting for the two-way coupling between the liquid and the bubbles is applied. We show that the model predicts accumulation of bubbles in thin sheets parallel to the walls. These singular structures, which are formally characterized by infinitely thin width and infinitely high concentration, are referred to as bubbly screens. The formation of a bubbly screen is described analytically in terms of a self-similar solution, which is in agreement with numerical simulations. We study the evolution of bubbly screens and detect a one-dimensional stationary state, which is shown to be unconditionally unstable.

I. INTRODUCTION

Bubbly liquid presents a well-known example of nonlinear medium [1]. The waves propagating through a bubbly liquid are able to display a variety of strongly nonlinear phenomena. Of particular interest is the averaged dynamics of periodically oscillating bubbly liquids. The equations governing the averaged dynamics of bubbly liquid have been developed by Kobelev and Ostrovsky [2]. A number of issues dealing with the propagation of acoustic waves in *unbounded* bubbly liquids have been addressed in Refs. [3–5]. From the perspective of applications and as a general aspect of pattern formation such factor as confinement becomes important, which particularly implies the consideration of standing waves. In our study, we focus on confined oscillating bubbly liquid and show that this system exhibits nontrivial highly localized states.

To the best of our knowledge, the averaged dynamics of bubbly liquid under confinement is first studied in Ref. [6], where a layer of bubbly liquid oscillating normally with respect to walls is considered. It has been numerically shown that the initially uniform state demonstrates an abrupt growth of the concentration field in one or several thin sheets parallel to the solid plates. However, the numerical solution does not allow us to clarify whether these structures develop into singular states within a finite time. The singular states can be referred to as *bubbly screens* as they are characterized by the vanishing width and infinite concentration of bubbles. Apart from the possibility of the bubbly screen formation, no analysis of their evolution has been performed. Additionally, we note that a bubbly screen can also be thought of as the

limit of an infinitely thin *bubble layer* with the infinite averaged concentration of bubbles [7–9].

To describe these singular objects one can employ the model describing a *dilute* monodisperse bubbly liquid [2,6]. In these models, one works in terms of an auxiliary field $\Phi = \phi/\epsilon$, which is the ratio of the volume fraction of bubbles $\phi = (4/3)\pi R^3 n \ll 1$ to an asymptotically small dimensionless problem-specific parameter $\epsilon \ll 1$. Here, n is the number of particles per unit volume of the medium and R is the time-averaged radius of a bubble. As a result, the rescaled field Φ is considered finite and can become large without a contradiction with the smallness of ϕ. For the sake of simplicity, Φ is referred to as the concentration. Furthermore, the vanishing width and the infinite value of the concentration are attributed to the bubbly screen only formally. In any real situation, these quantities are finite owing to certain factors such as interaction of bubbles and dissipative effects, which are usually not taken into account. Different ways are known to overcome this difficulty.

Although several papers deal with the collisions of bubbles via the calculation of the collision cross-section (see Ref. [2] and references therein), such approach does not seem convincing because various powers of the small ratio of the mean bubble radius to the mean interparticle distance are mixed. Another mechanism that allows one to prevent the infinite growth of the concentration is the diffusivity of bubbles [10]. On one hand, this diffusivity smears sharp spatial nonuniformities and stops the infinite growth of the concentration. As a result, the bubbly screen acquires a finite width and the maximum of concentration is no longer infinite. On the other hand, if not interested in resolving the structure of the bubbly screen, the description in terms of singular objects is possible. We stress that in contrast to the model of diffusive bubbly liquid [10], where the total amount of bubbles is kept constant as the bubbles can accumulate near the wall but cannot leave the system, the nondiffusive

*Author to whom correspondence should be addressed; straube@physik.hu-berlin.de
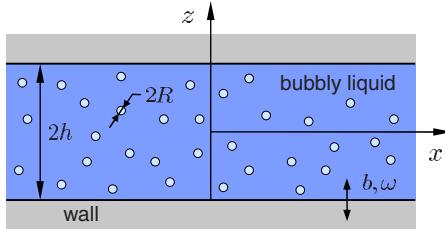
FIG. 1. (Color online) A sketch of the problem geometry. Bubbly liquid filling the space between solid parallel walls subject to normal oscillations with respect to the walls.

model is different. Mathematically, the flux of bubbles into the boundary is generally nonvanishing and the bubbles can leave the system. Physically, this fact suggests that the bubbles burst upon the contact with the wall. Another important distinction is that the stationary states are independent of initial conditions for diffusive bubbles [10], which is not the case in the present consideration.

In the present paper, we aim at studying the formation and evolution of the bubbly screens as singular objects. The analysis is performed for a layer of bubbly liquid confined by infinite solid plates. We start by formulating the problem in Sec. II. In Sec. III, we focus on the peaking regime and investigate the asymptotical behavior of the concentration field. The corresponding solution describes the formation of a bubbly screen. The evolution of the screen is studied in Sec. IV. We find a stationary solution that predicts that all the bubbles either settle at the walls or accumulate in the bubbly screens. These stationary states are shown to be unstable in Sec. V. The results are summarized in Sec. VI.

II. PROBLEM STATEMENT

Consider the averaged dynamics of a layer of dilute monodisperse bubbly liquid confined by the parallel solid plates separated by a distance $2h$. The system is subject to oscillations of an amplitude b and a frequency ω normally to the walls, as shown in Fig. 1.

To apply the model developed earlier (see, Sec. IV, Ref. [6]), we accept a number of assumptions. We assume the equilibrium radius of bubble R small compared to the size h. As was mentioned in Sec. I, we work in terms of the *finite* field $\Phi = \phi(h/R)^2$. Here, ϕ is the volume fraction of bubbles and the role of small parameter ϵ is played by $(R/h)^2 \ll 1$. We consider the oscillations to be small amplitude, $ah \ll R^2$, and high frequency, $\omega R^2 \gg \nu$. Here, ν is the kinematic viscosity of the liquid. For more general conditions that allow us to neglect the dissipation of bubble oscillations, see Ref. [11]. At the same time, the frequency ω is assumed small in the sense that $\omega h \ll c_0$, where c_0 is the speed of sound in the liquid free of bubbles. This requirement means that no acoustic waves are possible in the medium in the absence of bubbles.

For instance, the mentioned requirements are fulfilled for a 1% water ($\nu \simeq 10^{-2}$ cm^2 s^{-1}) suspension of bubbles with $R \simeq 3$ mm in a layer with $h \simeq 10$ cm, which oscillates with the amplitude $b = 10^{-3}$ cm and frequency $\omega = 10$ rad·s^{-1}.

Note that such choice of parameter values is in agreement with a typical vibration experiment, see e.g., Ref. [12].

We choose the Cartesian reference frame with the origin in the central plane of the layer, see Fig. 1. We measure the length, time, averaged and pulsation velocities, pressure, and bubble concentration in the scales of h, $h^2\nu^{-1}$, νh^{-1}, $b\omega$, $\rho\nu^2 h^2$, and $\phi_a h^2 R^{-2}$, respectively. Here, ρ is the liquid density and ϕ_a is the space-averaged volume fraction of the bubbles. As a result, the dimensionless boundary value problem is given by [cf. Eqs. (52)–(55) in Ref. [6]]

$$\partial_t \mathbf{u} + \mathbf{u} \cdot \nabla \mathbf{u} = -\nabla p + 3Q\Phi_a \Phi \nabla \psi^2, \tag{1a}$$

$$\partial_t \Phi + \text{div } \Phi \mathbf{u}_b = 0, \tag{1b}$$

$$\text{div } \mathbf{u} = 0, \quad \mathbf{u}_b = \mathbf{u} + Q \nabla \psi^2, \tag{1c}$$

$$\nabla^2 \psi + \frac{3\Phi_a \Phi(\mathbf{r})}{\Omega^2 - 1} \psi = 0, \tag{1d}$$

$$z = \pm 1 : \mathbf{u} = 0, \quad \mathbf{e}_z \cdot \nabla \psi = 1. \tag{2}$$

Here, $\mathbf{u}$ and $\mathbf{u}_b$ are the velocities of the liquid and bubble phases, respectively, p is the renormalized pressure, ψ is the amplitude of the velocity potential for the pulsation flow, and $\mathbf{e}_z = (0,0,1)$. Boundary conditions for Φ must be prescribed at the inflow boundaries, namely, if $\mathbf{u}_b \cdot \mathbf{e}_z > 0$ at $z = -1$ and if $\mathbf{u}_b \cdot \mathbf{e}_z < 0$ at $z = 1$. In this case we impose the vanishing flux of bubbles. At the outflow boundaries, no boundary conditions are required, which implies that the bubbles can settle on the walls. We assume that the settled bubbles burst and for this reason are no longer under consideration. Thus, the total amount of bubbles decreases, which is in contrast to the case of diffusive bubbles [10], where this quantity is conserved.

The problem is governed by the three dimensionless parameters,

$$Q = \frac{1}{\Omega^2 - 1} \left(\frac{b\omega h}{2\nu} \right)^2, \quad \Omega^2 = \frac{3\gamma P_g - 2\sigma R^{-1}}{\rho\omega^2 R^2},$$

$$\Phi_a = \phi_a \frac{h^2}{R^2},$$

where P_g, γ, and σ represent the mean pressure of the gas in bubbles, the adiabatic exponent, and the surface tension, respectively. The first parameter, Q, is proportional to the power of external driving and, for this reason, characterizes its intensity. The parameter Ω is the ratio of the eigenfrequency of the volume oscillations for a bubble to the frequency ω of external driving. The last parameter describes the feedback of bubbles on the liquid motion and rescales the concentration of bubbles. As ϕ_a is the small mean (space-averaged over the system) concentration of bubbles, the field Φ is normalized such that *initially* its space-averaged value equals one.

Consider the evolution of the initial state in the form of uniformly distributed bubbles and quiescent liquid and look for the one-dimensional solution. As the liquid remains motionless [6], $\mathbf{u}=0$, the boundary-value problem is reduced as follows:

$$\partial_t \Phi = -2Q\partial_z(\Phi\psi\partial_z\psi) = -\partial_z(u_b\Phi), \quad (3a)$$

$$\partial_z^2\psi = -\frac{3\Phi_a}{\Omega^2-1}\Phi\psi, \quad (3b)$$

$$z = 0: \partial_z\Phi = \psi = 0, \quad (3c)$$

$$z = 1: \partial_z\psi = 1, \quad (3d)$$

where the only nonvanishing is the z component of the bubble velocity, denoted as $u_b \equiv 2Q\psi\partial_z\psi$. Due to the symmetry of both boundary-value problem (3) and the initial conditions, we treat the problem in half the layer, $0 \leq z \leq 1$. Symmetry conditions (3c) imply that the concentration, Φ, and the potential, ψ, are even and odd functions of z, respectively.

Hereafter, we are interested in the case of low frequencies, $\Omega > 1$. For this consideration, we introduce the auxiliary parameter [6]

$$\alpha^2 = \frac{3\Phi_a}{\Omega^2-1}.$$

Without loss of generality, we can set $Q=1$ by the appropriate choice of the time scale, which is used in Secs. III and IV, where we explore the processes of formation and evolution of bubbly screens.

III. FORMATION OF BUBBLY SCREEN. PEAKING REGIME

As has been numerically detected earlier [6], the concentration of bubbles demonstrates an abrupt growth in one or a number of planes with $z=z_c$. We now demonstrate that this growth results in the development of a singular state at a certain moment of time t_0. To describe such state at times $t \approx t_0$ ($t < t_0$), a simple self-similar solution can be obtained.

Let us introduce the "fast" coordinate

$$\xi = \frac{z - z_c(t)}{\tau^{3/2}}, \quad \tau \equiv t_0 - t \ll 1 \quad (4)$$

and represent the fields of potential and concentration as superpositions

$$\psi = \Psi(z,t) + \tau^2 f(\xi,t), \quad \Phi = \frac{1}{\tau}F(\xi,t) + \phi(z,t), \quad (5)$$

where Ψ and ϕ are the regular parts of the fields and the functions f and F determine the self-similar contributions, respectively. Note that the leading term of the potential is given by the regular contribution, whereas for the concentration the self-similar term dominates. The function Ψ can be expanded into the Taylor series near z_c as follows:

$$\Psi(z \approx z_c, t) \approx \Psi_c(t) + (\partial_z\Psi)_c(z - z_c) + \cdots. \quad (6)$$

We substitute representations (5) and (6) into problem (3) and equate the terms of the same powers with respect to τ to obtain the differential equations

$$f'' + \alpha^2\Psi_c F = 0, \quad F + \frac{3}{2}\xi F' + 2\Psi_c(f'F) = 0 \quad (7)$$

and the relation

$$\dot{z}_c = 2\Psi_c(\partial_z\Psi)_c, \quad (8)$$

which describes the drift of the concentration peaks. Here, the primes and dot denote the ξ and t derivatives, respectively.

Equations (7) should be supplemented with the symmetry conditions

$$\xi = 0: f' = F' = 0. \quad (9)$$

Additionally, we can put $f(0)=0$, as only derivatives of f enter Eqs. (7).

The solution to the Cauchy problem given by Eqs. (7) and (9) can be presented in terms of an auxiliary function $y(\xi)$,

$$f = -\frac{1}{\Psi_c}\int_0^\xi y(\eta)d\eta, \quad F = \frac{y'(\xi)}{\alpha^2\Psi_c^2}. \quad (10)$$

The function $y(\xi)$ solves the nonlinear ordinary differential equation

$$(y^2)'' - \frac{3}{2}\xi y'' - y' = 0 \quad (11)$$

with the conditions

$$\xi = 0: y = 0, \quad y' = \frac{1}{2}, \quad (12)$$

where the second initial condition follows from Eq. (11) in view of the requirement $F'(0)=0$ or $y''(0)=0$.

Initial value problem (11) and (12) admits the nontrivial solution

$$\xi = 2y + 16By^3, \quad (13)$$

which leads to the following expressions for F and f:

$$F = \frac{1}{2\alpha^2\Psi_c^2(1 + 24By^2)}, \quad (14a)$$

$$f = \frac{y^2}{\Psi_c}(1 + 12By^2). \quad (14b)$$

It is worth noting that the Cauchy theorem is invalid for Eqs. (11) and (12). Indeed, by solving Eq. (11) with respect to y'', we obtain

$$y'' = 2y'\frac{1 - 2y'}{4y - 3\xi}. \quad (15)$$

Thus, accounting for Eq. (12) we see that both the numerator and denominator on the right-hand side of Eq. (15) vanish at $\xi=0$, which means the right-hand side of the equation is not
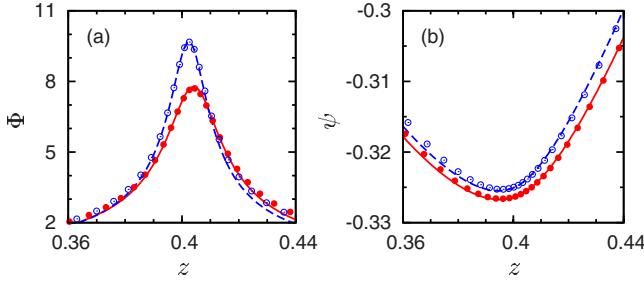
FIG. 2. (Color online) The comparison of numerical calculations (lines) and the asymptotic solution given by Eqs. (5), (13), and (14) (circles) presented for $\alpha^2=12$ ($t_0=0.401$). The concentration of bubbles (a) and velocity potential (b) at $t=0.350$ (solid lines and closed circles) and at $t=0.360$ (dashed lines and open circles).

continuous with respect to both ξ and y near the point $\xi=0$. This is why the Cauchy problem has a one-parameter family of solutions with B serving as the parameter.

At small ξ, when $y \approx \xi/2 - B\xi^3$, we arrive at the approximation

$$F = \frac{1 - 6B\xi^2}{2\alpha^2\Psi_c^2}, \quad f = -\frac{\xi^2(1 - B\xi^2)}{4\Psi_c}. \quad (16)$$

In the opposite case, $\xi \gg 1$, we obtain

$$F = -\frac{C}{3\alpha^2\Psi_c^2}\left(1 - \frac{2}{3}C\xi^{-2/3}\right)\xi^{-2/3}, \quad (17)$$

$$f = \frac{3C}{4\Psi_c}\left(1 + \frac{4}{3}C\xi^{-2/3}\right)\xi^{4/3}, \quad (18)$$

where

$$C^3 = -\frac{1}{16B}.$$

Thus, we see that F is finite at $\xi=0$ and at large ξ decays as $\xi^{-2/3}$, cf. Fig. 2(a). Therefore, the maximum of the concentration tends to infinity at $\tau \to 0$, see Eq. (5). At the same time, the width of this localized solution becomes vanishing. In other words, a δ-like distribution of the bubble concentration develops.

As follows from representation (5), the potential at $\tau \to 0$ is dominated by the regular contribution Ψ, which at z close to z_c corresponds to expansion (6). As the function $f(\xi)$ grows as $\xi^{4/3}$ at large ξ, the correction $\tau^2 f \propto (z - z_c)^{4/3}$ is smaller than the leading terms in Eq. (6), which ensures that the outer and the inner solutions are consistent and can be matched.

A comparison of numerical calculations and the asymptotic law, Eqs. (13) and (14), is illustrated in Fig. 2. In order to calculate the parameters Ψ_c, τ, and B included in self-similar solution (13) and (14), we compare the numerical data at two successive time moments, t_1 and t_2 such that $t_2 < t_1 < t_0$. Since the regular contribution to the concentration of the bubbles is rather small and varies slowly, we can assign $z_c(t_{1,2})$ such that $\Phi_{1,2} \equiv \Phi(z_c, t_{1,2}) = \max_z \Phi(z, t_{1,2})$. According to Eqs. (5) and (16), we have near the point z_c

$$\Phi \approx \frac{1}{2\alpha^2\Psi_c^2\tau}\left[1 - 6B\frac{(z - z_c)^2}{\tau^3}\right] + \phi_c, \quad (19)$$

where $\phi_c = \phi(z_c)$.

By comparing the numerically obtained values of $\Phi_{1,2}$ and $\partial_z^2\Phi$ at $z=z_c$ with those following from Eq. (19), we obtain

$$\tau = \frac{(t_1 - t_2)^2}{4} + \frac{t_1 - t_2}{2\Psi_c^2\alpha^2(\Phi_1 - \Phi_2)},$$

$$B = -\frac{\alpha^2}{6}\Psi_c^2\tau^4\partial_z^2\Phi,$$

where $\tau \equiv t_0 - (t_1 + t_2)/2$. Here, we have neglected variations of Ψ_c and ϕ_c (and, hence, B) with t, which leads to unimportant corrections of order $O(\tau)$. As a result, both Ψ_c and $\partial_z^2\Phi$ can be taken at either $t=t_1$ or $t=t_2$.

Next, we evaluate the velocity of the concentration maximum as $\dot{z}_c \approx [z_c(t_2) - z_c(t_1)]/(t_2 - t_1)$ and $(\partial_z\Psi)_c$ via Eq. (8). Finally, we have all necessary ingredients to approximate Ψ according to Eq. (6). As becomes clear from Fig. 2, good agreement of numerical data and the analytical solution is achieved even at $\tau \approx 0.0509$ ($t=0.350$).

IV. EVOLUTION OF BUBBLY SCREEN

A. Governing equations and boundary conditions

As we emphasized, at $t > t_0$ our model predicts unbounded accumulation of bubbles in thin sheets (or bubbly screens) with the coordinates $z = z_c$. Formally, $\Phi \to \infty$ in these planes and the model becomes inapplicable. As we mentioned in Sec. I, the proper treatment of such objects requires taking into consideration subtler factors such as bubble interactions and some dissipative effects. In this study, we resort to the approximation of diffusive bubbles [10]. This approximation, however, is rather a technical trick that helps in obtaining one of the matching conditions only and hence in completing the formulation of the model. As we are interested in the evolution of the bubbly screens and do not aim at resolving their structure, the developed model is kept nondiffusive and therefore operates by the bubbly screens as singular objects.

To study how the bubbly screen evolves, we represent the concentration field as a superposition of the regular contribution, ϕ, and a δ function,

$$\Phi = \phi + A(t)\delta(z - z_c(t)). \quad (20)$$

Here, $z = z_c(t)$ and $A(t)$ are respectively the position and "power" of the bubbly screen. The latter can be treated as $\lim_{\epsilon\to0}\int_{z_c-\epsilon}^{z_c+\epsilon}\Phi dz$. As for the potential, we can put $\psi = \Psi$. Indeed, although $\partial_z^2\psi$ diverges at $z=z_c$, the field itself, ψ, remains finite. Hence, the regular part of the potential, Ψ, coincides with ψ and no additional terms are required.

We note that the regular contributions to the solution, ϕ and Ψ, obey the same equations as before, see Eqs. (3) with ϕ and Ψ instead of Φ and ψ, respectively. To obtain the boundary conditions at the screen, we integrate Eqs. (3a) and (3b) over z from $z_c - \epsilon$ to $z_c + \epsilon$ and arrive at the expressions

$$\partial_t A - [\phi]V + 2\Psi[(\partial_z\Psi)\phi] = 0, \tag{21}$$

$$[\partial_z\Psi] + \alpha^2 A\Psi = 0, \tag{22}$$

where we have assumed that

$$[\Psi] = 0. \tag{23}$$

Here, the square brackets are used to denote the jump of the corresponding value across the screen

$$[g] \equiv g(z_c + \epsilon) - g(z_c - \epsilon)$$

and V is the velocity of the bubbly screen,

$$V \equiv \dot{z}_c,$$

which is yet to be determined. Note that the pair of boundary conditions, Eqs. (22) and (23), resembles the similar conditions at a δ-like potential in quantum mechanics [13].

To complete the set of boundary conditions at $z=z_c$ we need a relation that determines the velocity of the bubbly screen, V. To obtain such relation, we take infinitely small diffusion of bubbles into account in Eq. (3a) and end up with (the details are provided in Appendix A)

$$V = -\frac{[(\partial_z\Psi)^2]}{\alpha^2 A}. \tag{24}$$

Equations (21)–(24) present the full set of boundary conditions at $z=z_c$, which completes boundary-value problem (3) in the case of the bubbly screen emergence. We note that these additional boundary conditions can be easily included in the numerical algorithm applied earlier, see Sec. V of Ref. [6]. Therefore, we again apply the method of characteristics to numerically solve Eq. (3a) and the shooting method for Eq. (3b).

The initial conditions at $t=t_0$ correspond to $A=0$ and z_c is determined by extrapolation of the dependence $z_c(t)$ according to Eq. (8). Technically, we start the computation of the bubbly screen evolution at t slightly exceeding t_0, which is done to avoid the divergence of V, see Eq. (24) at $A=0$. As the initial distributions of Ψ and ϕ we use the fields ψ and Φ at $t \to t_0 - 0$ except at the close vicinity of the point $z=z_c$.

B. Numerical results and stationary solution

An example of computations for $\alpha^2=12$ is presented in Figs. 3 and 4. As can be seen from the figures, after the bubbly screen has formed, its power A monotonically increases. On the contrary, the regular part of the concentration ϕ tends to zero, which becomes clear from the evolution of

$$\langle\phi\rangle \equiv \int_0^1 \phi\,dz,$$

see Fig. 4(a). It is also worth noting that the potential Ψ becomes close to the piecewise-linear function that resembles the stationary solution obtained earlier in the limiting case of small diffusivity [10].

Recall that $u_b(z=1)>0$ for $\psi(z=1)>0$, which means that the flux of bubbles is positive at the solid wall, $z=1$, see Eq. (3a). Hence, a part of bubbles migrates toward the boundary,
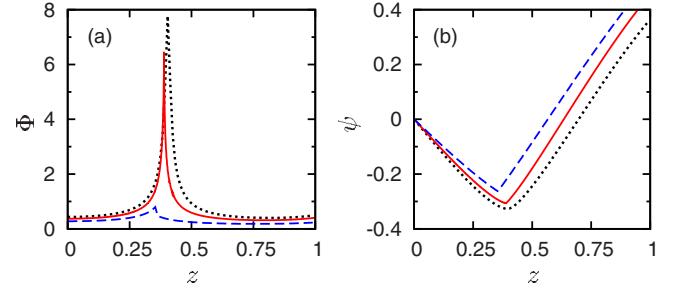

FIG. 3. (Color online) The fields of concentration Φ ($t<t_0=0.401$) or its regular part ϕ ($t>t_0$) (a) and velocity potential ψ (b) plotted for $\alpha^2=12$ at different times before and after the emergence of a bubbly screen. The dotted, solid, and dashed lines correspond to $t=0.35$, $t=0.425$, and $t=0.615$, respectively.

settles on it, bursts, and effectively disappears from the consideration. As a result, the total number of bubbles decreases even before the bubbly screen has formed [see the dashed-dotted line in Fig. 4(a)]. Thus, after a transient, all the bubbles either accumulate and compose the bubbly screen or disappear after settling on the solid wall. The system approaches the state described by the stationary solution

$$A = A_0, \quad z_c = \frac{2}{\alpha^2 A_0}, \quad \phi_0 = 0, \quad \psi_0 = |z - z_c| - z_c, \tag{25}$$

where $A_0 \leq 1$ is the fraction of bubbles that have formed the screen and therefore remained in the system. This quantity is determined by initial conditions and the value of α. For instance, for the solid wall repelling the bubbles, $u_b(z=1)<0$, no bubbles can leave the system and therefore $A_0=1$.

We stress that Eq. (25) is valid only within the range of frequencies Ω at which only one bubbly screen in half the layer, $0 \leq z \leq 1$, exists. A naive estimate of this frequency range in terms of α results in [cf. Eqs. (70) and (72) in Ref. [6]]

$$\pi/2 < \alpha < 3\pi/2. \tag{26}$$

For smaller values of α, all the bubbles leave the system, whereas for larger values of α, two or more screens emerge.
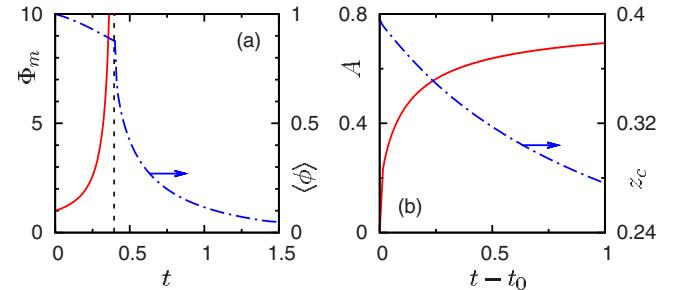

FIG. 4. (Color online) Evolution of the concentration plotted at $\alpha^2=12$ ($t_0=0.401$). Variation in maximal concentration, Φ_m (solid line) and mean value of concentration, $\langle\phi\rangle$ (dashed-dotted line) with t (a). The vertical dashed line shows the moment of formation of the bubbly screen, $t=t_0$. At $t>t_0$, only the regular part of the concentration, ϕ, contributes into $\langle\phi\rangle$. Characteristics of the bubbly screen (b): the power A (solid line) and position z_c (dashed-dotted line).

The generalization of Eq. (25) for the case of several bubbly screens is straightforward.

In fact, criterion (26) for the formation of a single screen is not rigorous. For instance, our numerical simulations performed at $\alpha^2 = 1.9$ and $\alpha^2 = 2$ (for both cases $\alpha < \pi/2$) show the formation of a single screen. Here, the bubbles initially tend to reach the boundary, which is accompanied by the decrease in the total number of bubbles. However, significant changes in the concentration field lead to a crossover. After the movement toward the wall, the bubble flux at the wall becomes negative and the bubbles start to move backward, away from the wall. As a result, a band of pure liquid is formed near the wall. With the time, this band expands away from the wall, cf. Fig. 6 in Ref. [6].

Mathematically, the appearance of the crossover can be associated with the dynamics of the potential, ψ, which first tends to infinity and then changes its sign at $t = t_*$. Note that the infinite value of ψ means that at a given α, the Helmholtz equation, Eq. (3b), has a nontrivial solution with the zero flux at the boundaries, $\partial_z \psi(z=1) = 0$ for a certain distribution of bubbles $\Phi_*(z) = \Phi(z, t_*)$. Physically, a kind of resonance occurs as one of the eigenfrequencies for the instantaneous distribution of bubbles coincides with the frequency of oscillations. Interestingly, the evolution at $\alpha^2 = 1.8$ is similar to the described scenario but not the same. At the initial stage the bubbles move toward the wall. However, the process of sedimentation of the bubbles on the wall is so fast that no crossover occurs: after the transient, the maximum of the potential starts to decrease before reaching the infinite value.

On the other hand, the study involving diffusivity of bubbles [10] claims that n bubbly screens in half the layer exist provided that $2n(2n-1) < \alpha^2 < (2n+1)(2n+2)$. We emphasize that this result is inappropriate for the problem under consideration. The reason is that in the presence of bubble diffusivity, the steady state does not depend on the initial conditions, whereas in the present nondiffusive study it does.

Sooner or later, in each half the layer the bubbles symmetrically form one or several bubbly screens. The system arrives at the steady state in which every screen is described by Eq. (25). The value of A_0 is to be figured out numerically. Thus, the next question to answer is whether the detected stationary state is stable.

V. STABILITY OF THE STATIONARY STATE

In this section we explore the stability of the stationary state obtained in Sec. IV. Although the stationary state is one dimensional, the stability analysis requires the three-dimensional generalization of the governing equations, which is provided in Appendix B. For the sake of simplicity, we deal with the case of a single bubbly screen in half the layer, see Eq. (25).

We introduce small perturbations of the power of the bubbly screen, a, its position, ζ, potential of pulsations, Ψ, averaged velocity, $\mathbf{U}$, pressure, P, and background concentration of the bubbles, c. After the linearization with respect to small perturbations we arrive at the boundary-value problem

$$\partial_t \mathbf{U} = -\nabla P + \nabla^2 \mathbf{U} + 3Q\Phi_a(\psi_0^2)' c \mathbf{e}_z, \tag{27}$$

$$\nabla \cdot \mathbf{U} = 0, \tag{28}$$

$$\partial_t c = -2Q\partial_z(c\psi_0\psi_0'), \tag{29}$$

$$\nabla^2 \Psi = -\alpha^2 \psi_0 c, \tag{30}$$

$$z = \pm 1 : \mathbf{U} = \partial_z \Psi = 0, \tag{31}$$

where the primes denote the derivatives with respect to z. Owing to O_2 symmetry in the plane (x, y), we restrict our analysis by the two-dimensional consideration. We set $U_y = 0$, and $\partial_y \equiv 0$.

Because of symmetry, it is convenient to treat this problem in half the layer, $0 \leq z \leq 1$. At $z = 0$, we impose the symmetry conditions, which correspond to either

$$U_z = \partial_z U_x = \Psi = \partial_z c = 0 \tag{32}$$

for *odd* perturbations or

$$U_x = P = \partial_z \Psi = c = 0 \tag{33}$$

for *even* perturbations. Here, we bear in mind that in the former case the functions Ψ and U_z are odd, whereas U_x, P, and c are even and vice versa for the latter case.

The matching conditions are formulated at the unperturbed bubbly screen, $z = z_c$,

$$\partial_t a = -A_0 \partial_x \{U_x + 2Q\psi_0 \partial_x(\Psi + \psi_0'\zeta)\} + 2Q\psi_0[c\psi_0'], \tag{34a}$$

$$[\Psi] = -2\zeta, \tag{34b}$$

$$[\partial_z \Psi] = -\alpha^2 \{\psi_0 a + A_0(\Psi + \psi_0'\zeta)\}, \tag{34c}$$

$$[\mathbf{U}] = 0, \quad [P] = -\frac{6Q}{\alpha^2}\Phi_a[\psi_0'\partial_z\Psi], \tag{34d}$$

$$[\partial_x U_z] = -[\partial_z U_x] - 6Q\Phi_a ikA_0\psi_0(\Psi + \psi_0'\zeta), \tag{34e}$$

$$\partial_t \zeta = U_z - \frac{2Q}{\alpha^2 A_0}[\psi_0'\partial_z\Psi]. \tag{34f}$$

It is clear that the boundary-value problem for c can be decoupled from the other equations. We note that the space-averaged concentration $\langle c \rangle$ decays in time, which means that this mode does not lead to instability. For this reason, hereafter we set $c = 0$.

To separate the time and x dependencies, we consider the normal modes. Accordingly, the fields of perturbations are presented as $g(x, z, t) = \hat{g}(z)\exp(\lambda t + ikx)$, where λ and k are the complex growth rate and the wave number, respectively. We introduce the stream function φ by the relations, $\hat{U}_x = -\hat{\varphi}'$, $\hat{U}_z = ik\hat{\varphi}$, and obtain for the complex amplitudes

$$\hat{D}^2(\hat{D}^2 - \lambda)\hat{\varphi} = 0, \tag{35a}$$

$$\hat{D}^2\hat{\Psi} = 0, \tag{35b}$$

$$z = 1: \hat{\varphi} = \hat{\varphi}' = \hat{\Psi}' = 0, \tag{35c}$$

where $\hat{D}^2 = d^2/dz^2 - k^2$ is the Fourier image of the Laplace operator. The symmetry and matching conditions straightforwardly follow from Eqs. (32)–(34) and are not presented here. It is important that Eqs. (35) are not coupled to each other and therefore their solutions are easily found. The fields of perturbations in the general case of arbitrary k are presented in Appendix C. Here we deal with two limiting cases that admit analytical solutions.

In the "shortwave" limit, $k \gg 1$, both the symmetry conditions at $z=0$ and the conditions at the wall, $z=1$, become unimportant. Instead, we only need to ensure that the perturbations decay far away from the bubbly screen. Furthermore, in Eq. (35a) we can neglect the term $\propto \lambda$ in comparison with k^2. Note, however, that the similar term in Eq. (34a) must be retained. As a result, we obtain

$$\hat{\varphi}_{\pm} = (C_{\pm} + ZD_{\pm})e^{\mp kZ}, \quad \hat{\Psi}_{\pm} = B_{\pm}e^{\mp kZ}, \tag{36}$$

where $Z \equiv z - z_c$ and "+" and "−" correspond to the domains $Z > 0$ and $Z < 0$, respectively. Matching these solutions at the bubbly screen, we obtain a set of eight linear algebraic equations for $B_{\pm}$, $C_{\pm}$, $D_{\pm}$, $\hat{\zeta}$, and $\hat{a}$. This system has two kinds of solutions,

(i) $\hat{\zeta} \neq 0$, $C_{\pm} = kC + O(1)$, $B_+ \neq B_-$ with the negative growth rate

$$\lambda = -Q\left(2kz_c + \frac{3\Phi_a}{\alpha^2}\right) \approx -2Qkz_c, \tag{37}$$

and

(ii) $B_- = B_+$, $\hat{\zeta} = C_{\pm} = 0$ with the positive growth rate

$$\lambda = Qkz_c\frac{4k - 3A_0\Phi_a}{2k - \alpha^2 A_0} \approx 2Qkz_c. \tag{38}$$

Thus, the one-dimensional state is unconditionally unstable, at least with respect to the shortwave mode.

Another interesting limit corresponds to the case $\Phi_a = 0$. In this case, the averaged liquid motion and the deformation of the bubbly screen decouple. Indeed, the evolution of $\hat{\varphi}$ is described by a separate boundary-value problem, which is known to predict monotonic decay of the velocity perturbations (or "hydrodynamic" modes) [15]. So we set $\hat{\varphi} = 0$ and pay attention to the boundary-value problem for $\hat{a}$, $\hat{\zeta}$, and $\hat{\Psi}$. For this mode, the growth rate λ obeys a quadratic equation with cumbersome coefficients, which is not presented here. The variation in λ with k is shown in Fig. 5. Note that for $\Phi_a = 0$ the growth rate is proportional to Q and depends on the product $\alpha^2 A_0 = 2/z_c$ rather than on each of the parameters, A_0 and α, separately.

It is important that $\lambda \to \infty$ at a certain value $k = k_*$. This value is determined by the transcendental equations

$$\Gamma_+(k_*) + \Gamma_-^{(e,o)}(k_*) = 2, \tag{39}$$

where
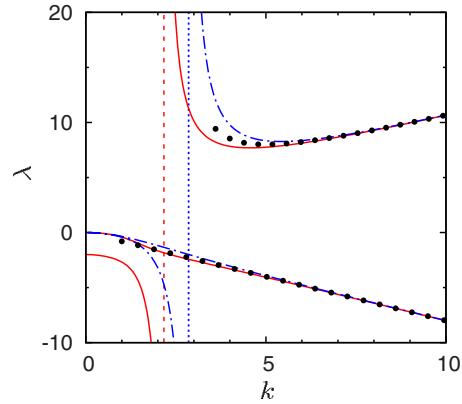
$$\Gamma_+(k) \equiv kz_c \tanh k(1 - z_c),$$

FIG. 5. (Color online) Growth rates λ as a function of k plotted for $\Phi_a = 0$, $Q = 1$, $A_0\alpha^2 = 5$. The solid and dashed-dotted lines correspond to the odd and even modes, respectively. Vertical asymptotes are determined by Eqs. (39). Asymptotical formulas (37) and (38), are shown by circles.

$$\Gamma_-^{(e)}(k) \equiv kz_c \tanh kz_c, \quad \Gamma_-^{(o)}(k) \equiv kz_c \coth kz_c$$

and the superscripts "e" and "o" stand for the even and odd modes, respectively. Consider the eigenvalue problem determined by

$$\hat{D}^2\hat{\Psi} = 0, \tag{40a}$$

$$z = 1: \hat{\Psi}' = 0, \tag{40b}$$

$$z = z_c: [\hat{\Psi}] = 0, \quad [\hat{\Psi}'] + \alpha^2 A_0 \hat{\Psi} = 0, \tag{40c}$$

$$z = 0: \hat{\Psi}^{(e)\prime} = \hat{\Psi}^{(o)} = 0, \tag{40d}$$

where Eqs. (40a)–(40c) are valid for both $\hat{\Psi}^{(e)}$ and $\hat{\Psi}^{(o)}$.

At $k = k_*$, which plays the role of the eigenvalue, this problem has a nontrivial solution given by Eqs. (C1) and (C2) with $B_+ = B_-$. Physically, the obtained solution describes excitation of a wave in the layer of bubbly liquid with a δ-like distribution of bubbles. In fact, Eq. (39) serves as a dispersion relation for this wave and ensures that its eigenfrequency coincides with the external frequency Ω. This coincidence, however, does not lead to the resonant amplification of the base state. The reason is that the external driving is independent of x, which means that it corresponds to $k = 0$ and has vanishing projection onto the eigenmode with $k = k_*$. From the mathematical point of view, the existence of the nontrivial solution of the Laplace equation follows from the unusual form of the matching condition, Eq. (40c).

While considering the solutions with the wave number k close to the eigenvalue k_*, we can expect *resonant* phenomena. At $k \approx k_*$, both $\hat{a}$ and $\hat{\zeta}$ are of order $O(k-k_*)$. The growth rate is evaluated to yield

$$\lambda \approx \frac{\beta Q}{k - k_*}, \quad \beta = \frac{(\Gamma_+ - \Gamma_-)^2 + (2k_* z_c)^2}{\dfrac{\partial(\Gamma_+ + \Gamma_-)}{\partial k}} > 0,$$

where the functions $\Gamma_\pm$ and their derivatives are taken at $k = k_*$ and Γ_- is for either even or odd mode. As β is positive, we conclude that at $k = k_* + 0$ the perturbation grows infinitely fast. At $k < k_*$, the corresponding mode is stable, $\lambda(k < k_*) < 0$. Furthermore, the similar divergence of λ at $k \approx k_*$ occurs for $\Phi_a \neq 0$.

Note that except for the shortwave instability, the obtained spectrum resembles the one found out in a similar study, see Fig. 7 in Ref. [10]. At first glance, this similarity is quite unexpected as we investigate the stability of completely different base states: an almost uniform distribution of bubbles in Ref. [10] and a highly nonuniform δ-like distribution in the present study. However, a closer comparison of the stability problems reveals the same resonant phenomenon behind the instability. In both situations, it originates from the nontrivial solution of the boundary-value problem for the potential at a given distribution of bubbles—spatially homogeneous as in the diffusive study [10] or a δ-like as in the present work. This nontrivial solution, whose eigenfrequency coincides with Ω, exists only at the resonant value of the wave number ($k = \alpha$ in Ref. [10] and $k = k_*$ here). At this value, the growth rate has a pole and hence diverges, which causes similar behavior of λ near the resonant value of the wave number in the two problems.

Finally, we emphasize that the variation in parameters does not lead to qualitative change in the spectrum. The increase in Φ_a weakly diminishes λ, but the vertical asymptotes at $k = k_*$ and the asymptotic behavior at $k \to \infty$ remain unchanged. Larger values of both A_0 and α^2 result in stretching along k of all the curves $\lambda(k)$ shown in Fig. 5. The increase in Q basically stretches the curves along the λ-axis. Thus, the one-dimensional bubbly screen is found to be unstable.

VI. SUMMARY

We have studied the dynamics of a dilute monodisperse bubbly liquid confined by a pair of plane solid walls, which are subject to small-amplitude high-frequency oscillations normally to the walls. The period of these oscillations is assumed small in comparison with typical relaxation times for a single bubble. At the same time, we focus on the case of low frequencies, where the ratio Ω of the eigenfrequency of volume oscillations to the frequency of external driving, is considered to be $\Omega > 1$. We apply the time-averaged description accounting for the two-way coupling between the liquid and the bubbles and analyze the formation and evolution of the one-dimensional states in the form of bubbly screens. The initial state corresponds to the uniform distribution of bubbles and motionless liquid.

We have shown that the model predicts accumulation of bubbles in a single or several pairs of planes between the confining walls. The corresponding singular structures of infinitely thin width and infinitely high concentration are referred to as bubbly screens. The peaking regime that corre-

sponds to the formation of a bubbly screen can be described in terms of a self-similar solution. This problem is reduced to a nonlinear ordinary differential equation that admits an analytical solution. We have demonstrated that this solution is in good agreement with the results of numerical simulations.

We have studied the evolution of the bubbly screens and detected a one-dimensional stationary state. This solution implies that all the bubbles either settle on the walls or accumulate in eventually motionless bubbly screens. We have explored the stability of this stationary state and arrived at the conclusion that this one-dimensional stationary state is unconditionally unstable. We note that except for the shortwave instability, the spectrum of growth rates is reminiscent of that found out in a recent study, see Fig. 7 in Ref. [10]. This similarity can be explained by the excitation of a standing sound wave with the eigenfrequency Ω and a certain (eigen or resonant) value of the wave number. At this value of the wave number, the growth rate has a pole and for this reason demonstrates similar divergence.

APPENDIX A: SOLUTION IN THE LIMIT OF SMALL BUBBLE DIFFUSIVITY

To derive the equation that determines the velocity of the bubbly screen, V, we provisionally take into account the diffusivity of bubbles. In Eq. (3a), we add a diffusion term with a small dimensionless coefficient of diffusion D, which has the meaning of the inverse Schmidt number S [10]. Although usually $S \gg 1$, the diffusive term must be retained in the thin layer close to the bubbly screen. By introducing the fast coordinate $\xi \equiv (z - z_c)/D$, we represent the fields inside the transition layer as follows:

$$\psi = \Psi_c + D f(\xi), \quad \Phi = D^{-1} F(\xi) + \phi(z, t). \quad (A1)$$

Here, $\Psi_c = \Psi(z = z_c)$ is a constant value. By substituting decomposition (A1) into Eqs. (3), to the leading orders we obtain

$$f'' + \alpha^2 \Psi_c F = 0, \quad (A2)$$

$$-F'V + 2\Psi_c(f'F)' = F'', \quad (A3)$$

where the primes denote the derivatives with respect to ξ.

The integration of Eq. (A3) over ξ yields

$$F' = -FV + 2\Psi_c f' F,$$

where the constant of integration is set to zero, because both F and F' vanish as $\xi \to \infty$.

We integrate this relation from $\xi = -\infty$ to $\xi = +\infty$ and obtain

$$VA = 2\Psi_c \int_{-\infty}^{+\infty} f' F d\xi, \tag{A4}$$

where we have taken into account the definition of the screen power

$$\int_{-\infty}^{+\infty} F d\xi = \int_{z_c - \epsilon}^{z_c + \epsilon} \Phi dz = A.$$

To evaluate the right-hand side of Eq. (A4), we multiply Eq. (A2) by $2f'$ and integrate, which results in

$$2\alpha^2 \Psi_c \int_{-\infty}^{+\infty} f' F d\xi = -(f')^2|_{-\infty}^{+\infty} = -[(\psi')^2]. \tag{A5}$$

Here we postulate a relation between the outer and inner solutions

$$\partial_z \Psi(z = z_c \pm \epsilon) = f'(\xi = \pm \infty).$$

Finally, we substitute Eq. (A5) into Eq. (A4) and arrive at Eq. (24). Note that the final expression is independent of D.

APPENDIX B: GENERALIZATION OF THE MODEL FOR THREE DIMENSIONS

We now generalize our model for three dimensions. We start by considering the phase of the formation of the bubbly screen, $t < t_0$. We assume that the bubbly screen forms at a certain "protoscreen" surface $G(\mathbf{r}, t) = 0$, at which the concentration of bubbles tends to infinity. As in the one-dimensional consideration in Secs. III and IV, we are interested in the description of the formation and evolution of the bubbly screen.

First of all, we outline the equations that describe the formation of the bubbly screen. Note that in contrast to the previous sections, no reason exists to neglect the liquid flow in the three-dimensional consideration. As a result, along with the fields of potential ψ and concentration of bubbles Φ, we have to retain the liquid velocity, $\mathbf{u}$. For this reason, we can no longer apply the condition $Q = 1$, which was accepted in Secs. III and IV.

We introduce the fast coordinate ξ in the same way as in Eq. (4), where z is now the coordinate normal to the (locally flat) surface $G = 0$, and represent the concentration and potential in the form given by Eqs. (5). We note that the liquid velocity is presented by the regular part only: as it can be easily shown, the ξ-dependent part of $\mathbf{u}$ is $o(\tau^2)$.

Thus, the only significant distinction to the one-dimensional case is that Ψ now varies along the protoscreen surface. Nevertheless, Eqs. (7) and the solution, Eqs. (13) and (14), remain valid. Although the increase in Φ is nonuniform along the surface $G = 0$, the concentration of bubbles becomes infinite simultaneously in all the points of this surface.

The drift of the protoscreen surface is described by the kinematic condition

$$\partial_t G + \mathbf{u}_b \cdot \nabla G = 0, \quad \mathbf{u}_b = \mathbf{u} + Q \nabla (\Psi)^2,$$

which now replaces Eq. (8). Such replacement is quite expected as the drift velocity of the concentration maximum is determined by the local velocity of bubbles.

By the time $t = t_0$, the bubbly screen has formed and we proceed to the consideration of its evolution, $t > t_0$. Let a bubbly screen of power $A(\mathbf{r}, t)$ emerge at the surface $G(\mathbf{r}, t) = 0$. Using the same approach as in Sec. IV A, we arrive at the following set of boundary conditions valid at this surface:

$$\partial_t A + \nabla_\tau \cdot (A \mathbf{u}_{b\tau}) + VA \nabla_\tau \cdot \mathbf{n} = (V - u_n)[\phi] - 2Q\psi[\phi \nabla_n \psi], \tag{B1}$$

$$[\psi] = 0, \quad [\nabla_n \psi] = -\alpha^2 \psi A, \tag{B2}$$

$$V = u_n - \frac{Q}{\alpha^2 A}[(\nabla_n \psi)^2], \tag{B3}$$

$$[\mathbf{u}] = 0, \quad [T_{n\tau}] = -6Q\Phi_a A\psi \nabla_\tau \psi, \tag{B4}$$

$$-[p] + [T_{nn}] = \frac{3Q}{\alpha^2} \Phi_a [(\nabla_n \psi)^2]. \tag{B5}$$

Here, the subscripts τ and n denote the tangential and normal components of the corresponding quantities, T is the viscous stress tensor, and V is the normal component of the bubbly screen velocity. The sign of the normal $\mathbf{n}$ to the bubbly screen and the jump across the screen are related to each other as follows: for a jump $[g] = g_2 - g_1$, the normal vector is directed from domain 1 to domain 2.

As we can see from the generalized model, the curved bubbly screen contributes into both the normal and tangential stresses. The most interesting is the role of the effectively generated tangential drag on the liquid, which is caused by the variation in ψ along the bubbly screen and therefore resembles the Marangoni drag along a nonuniformly heated interface [14].

APPENDIX C: PARTIAL SOLUTIONS OF THE STABILITY PROBLEM

For an arbitrary value of k, the solution for the potential can be presented as

$$\hat{\Psi}_+ = B_+ \frac{\cosh kz_1}{\cosh k(1 - z_c)}, \quad z_1 = 1 - z \tag{C1}$$

at $z > z_c$ and

$$\hat{\Psi}_-^{(e)} = B_- \frac{\cosh kz}{\cosh kz_c}, \quad \hat{\Psi}_-^{(o)} = B_- \frac{\sinh kz}{\sinh kz_c} \tag{C2}$$

at $z < z_c$. Here, again, the superscripts "e" and "o" refer to the even and the odd mode, respectively.

The stream function is found to be

$$\hat{\varphi}_+ = C_+ \frac{q \sinh kz_1 - k \sinh qz_1}{k \sinh k(1 - z_c)} + D_+ \frac{\cosh kz_1 - \cosh qz_1}{\cosh k(1 - z_c)} \tag{C3}$$

at $z > z_c$ and

$$\hat{\varphi}_-^{(e)} = C_- \frac{\cosh kz}{\cosh kz_c} + D_- \frac{\cosh qz}{\cosh qz_c}, \tag{C4}$$

$$\hat{\varphi}_-^{(o)} = C_- \frac{\sinh kz}{\sinh kz_c} + D_- \frac{\sinh qz}{\sinh qz_c} \tag{C5}$$

at $z < z_c$. Here, $q^2 = k^2 + \lambda$.

These solutions satisfy Eqs. (35) and the boundary conditions at the plane of symmetry, $z = 0$, and at the solid wall, $z = 1$. The substitution of these solutions into the matching conditions at the bubbly screen, Eqs. (34), results in a system of eight linear homogeneous algebraic equations for $B_\pm$, $C_\pm$, $D_\pm$, $\hat{\zeta}$, and $\hat{a}$. The requirement of the vanishing determinant provides an algebraic equation for λ, which is solved numerically.

[1] K. A. Naugolnykh and L. A. Ostrovsky, *Nonlinear Wave Processes in Acoustics* (Cambridge U.P., New York, 1998).

[2] Yu. A. Kobelev and L. A. Ostrovsky, J. Acoust. Soc. Am. **85**, 621 (1989).

[3] I. Akhatov, U. Parlitz, and W. Lauterborn, J. Acoust. Soc. Am. **96**, 3627 (1994).

[4] U. Parlitz, C. Scheffczyk, I. Akhatov, and W. Lauterborn, Chaos, Solitons Fractals **5**, 1881 (1995).

[5] I. Akhatov, U. Parlitz, and W. Lauterborn, Phys. Rev. E **54**, 4990 (1996).

[6] A. V. Straube, D. V. Lyubimov, and S. V. Shklyaev, Phys. Fluids **18**, 053303 (2006).

[7] O. A. Druzhinin, L. A. Ostrovsky, and A. Prosperetti, J. Acoust. Soc. Am. **100**, 3570 (1996).

[8] L. A. Ostrovsky, A. M. Sutin, I. A. Soustova, A. I. Matveyev, and A. I. Potapov, J. Acoust. Soc. Am. **104**, 722 (1998).

[9] S. Karpov, A. Prosperetti, and L. Ostrovsky, J. Acoust. Soc. Am. **113**, 1304 (2003).

[10] S. Shklyaev and A. V. Straube, Phys. Fluids **21**, 063303 (2009).

[11] L. V. Wijngaarden, Annu. Rev. Fluid Mech. **4**, 369 (1972).

[12] V. G. Kozlov, A. A. Ivanova, and P. Evesque, Europhys. Lett. **42**, 413 (1998).

[13] S. Flügge, *Practical Quantum Mechanics* (Springer, Berlin, 1994).

[14] A. A. Nepomnyashchy, M. G. Velarde, and P. Colinet, *Interfacial Phenomena and Convection* (Chapman and Hall, London /CRC, Boca Raton, 2001).

[15] G. Z. Gershuni and E. M. Zhukhovitsky, *Convective Stability of Incompressible Fluid* (Keter, Jerusalem, 1976).